Distribution Agreement

In presenting this thesis or dissertation as a partial fulfillment of the requirements for an advanced degree from Emory University, I hereby grant to Emory University and its agents the non-exclusive license to archive, make accessible, and display my thesis or dissertation in whole or in part in all forms of media, now or hereafter known, including display on the world wide web. I understand that I may select some access restrictions as part of the online submission of this thesis or dissertation. I retain all ownership rights to the copyright of the thesis or dissertation. I also retain the right to use in future works (such as articles or books) all or part of this thesis or dissertation.

Signature:

_____ _____

Lan Ge Date

Development of High Throughput Screening Methods
to Identify Potential Therapeutic Oxygen Carriers

By

Lan Ge
Master of Science

Chemistry

_____

Emily Weinert, Ph.D.
Advisor

_____

Justin Gallivan, Ph.D.
Committee Member

_____

Stefan Lutz, Ph.D.
Committee Member

Accepted:

_____

Lisa A. Tedesco, Ph.D.
Dean of the James T. Laney School of Graduate Studies

_____

Date

Development of High Throughput Screening Methods to Identify Potential Therapeutic Oxygen Carriers

By

Lan Ge
B.S., Hunan University, 2011

Advisor: Emily Weinert, Ph.D.

An abstract of
A thesis submitted to the Faculty of the
James T. Laney School of Graduate Studies of Emory University
In partial fulfillment of the requirements for the degree of
Master of Science
In Chemistry
2013

Abstract

Development of High Throughput Screening Methods
to Identify Potential Therapeutic Oxygen Carriers

By Lan Ge

Blood shortage has become a worldwide problem in recent years, caused by the increased demand for blood transfusions and reduced supply of healthy blood. To address this problem, hemoglobin-based blood substitutes have been previously designed, but challenges still remain due to their instability under physiological conditions. Recently, a class of heme proteins, Heme-Nitric oxide/OXygen binding domains from *Thermoanaerobacter tengcongensis* (*Tt* H-NOX), with tunable oxygen affinity and extraordinary stability has been considered as a promising candidate for therapeutic oxygen delivery. Previous studies have focused on engineering the oxygen binding affinity of *Tt* H-NOX by performing site directed mutagenesis on its active site. However, given limited knowledge beyond the active site and the time required for characterization, more effective methods need to be developed for blood substitute development. Therefore, directed evolution and high throughput screening approach was developed in this study. To remove non-heme bound proteins potentially evolved from directed evolution, a high throughput heme incorporation assay was developed, which select for heme-bound proteins in whole cells. In addition, multiple optical based medium throughput oxygen affinity assays were developed. By correlating the oxygen dissociation constant of the protein with the luminescence or fluorescence output, the protein's oxygen affinity were optically measured in 96-well plates. To validate these developed assays, a site saturation library of *Tt* H-NOX was generated at Y140, L144, G71 and G143 sites, which can be screened for useful properties for therapeutic oxygen delivery. These studies will also highlight residues outside the heme active site that are important for modulating oxygen affinity.

Development of High Throughput Screening Methods to Identify Potential Therapeutic Oxygen Carriers

By

Lan Ge
B.S., Hunan University, 2011

Advisor: Emily Weinert, Ph.D.

A thesis submitted to the Faculty of the
James T. Laney School of Graduate Studies of Emory University
In partial fulfillment of the requirements for the degree of
Master of Science
In Chemistry
2013

Table of Contents

Index of Figures

Index of Tables

Introduction

Blood Shortage

In recent years, the worldwide reduction of blood reserves has generated new challenges in human medicine. In developed countries, due to the growth of aging population, a major blood shortage of 4 million units has been projected by the year 2030.[1] In developing countries, infectious diseases such as malaria and HIV, together with limited clinical treatment conditions, have made the blood transfusion process severe and compromised.[2] According to a recent report of the World Health Organization (WHO), the low quality of blood transfusion has become a non-negligible factor causing human death in third world countries.[3] Much effort has been put towards solving this urgent health related problem and the search for an artificial blood alternative has emerged as an active area of research.[4]

Heme Proteins

Most of the artificial blood research has focused on creating a therapeutic oxygen carrier, rather than a true blood substitute, since the most important feature of blood cells is oxygen delivery.[5] In human body, natural oxygen carriers are hemoglobin (Hb) and myoglobin (Mb), which delivers oxygen in blood and muscles respectively. Their oxygen binding affinity varies significantly as they function in different cell types. For example, at 37°C, the p50 of Hb is 26 Torr (K_d = 26 μM), which is suitable for O_2 to be delivered to tissues.[6] While Mb has a p50 of 2.5 Torr (K_d = 2.5 μM) under the same condition, and Mb-bound O_2 can be used in the energy generation to fuel muscle contraction.[7]

Both Hb and Mb contain an iron-centered, hydrophobic, protoporphyrin IX cofactor, known as heme (Figure 1). With the incorporation of the heme cofactor, proteins have evolved variety of functions such as catalysis, electron transfer and gas sensing.[8] Specifically, when the central heme iron is in the ferrous state, some of heme proteins display ligand affinity for diatomic gases such as nitric oxide (NO), oxygen (O_2), and carbon monoxide (CO).[9] This gaseous ligand affinity enables heme proteins to play an indispensable role in regulating physiological activities in animals, plants and bacteria.[9-10]

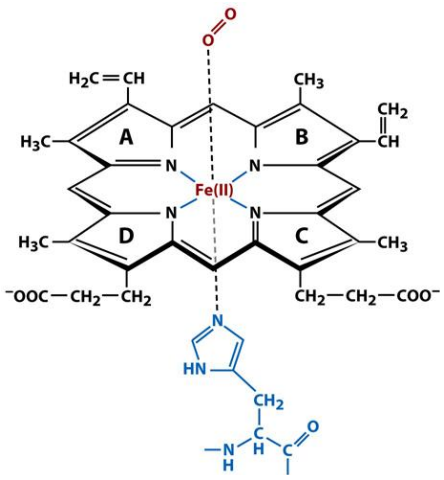

Figure 1: Structure of heme [11]

Since Hb and Mb have evolved to serve as O_2 carriers, they have been targeted as artificial blood substitutes for oxygen delivery.[5, 12] However, many difficulties still remain unaddressed. For instance, when Hb is not protected by red blood cells, it can be easily oxidized to its ferric state, forming methemoglobin (MetHb) that is incapabale of oxygen binding and delivery.[13] Also, cell-free Hb serves as strong NO scavenger with a high rate of NO consumption, which restricts NO bioavailability.[14] Due to the depletion

of NO, blood pressure might increase by vasoconstriction, accompanied by decrease in the heart rate.[15]

To overcome the challenges of Hb-based oxygen carriers, alternative sources of artificial therapeutic oxygen carriers such as fluorocarbons (PFCs) are being considered.[16] However, because the complicated blood circulation system requires the candidate to be stable, biocompatible and capable of oxygen delivery, heme proteins of tunable oxygen affinity still remain as preferable choices.[4]

The H-NOX Family of Heme Proteins

Heme-Nitric oxide/OXygen binding (H-NOX) proteins comprise a family of heme protein sensors conserved from bacteria to human beings.[17] The H-NOX domain contains a protoporphyrin IX heme and has evolved to bind gaseous ligands. The predicted H-NOX proteins are all about 190 amino acids in length with significant sequence homology (15–40% identity).[18] The heme group interact with the heme pocket through van der Waals interaction as well as the ligand binding between its heme-iron and a proximal histidine, which is conserved in all H-NOX domains.[19] Although similar in structure, these H-NOX domains display divergent ligand discrimination and affinity based on native organisms. For example, soluble guanylate cyclase (sGC), which is found in mammals, contains an H-NOX domain and functions as mammalian NO receptor, exhibiting picomolar binding constants for NO, with no measurable O_2 affinity.[20] Although the function of bacterial H-NOX domains are not well understood, studies suggest that some of them function as NO sensors to regulate cellular responses such as biofilm formation and quorum sensing.[21] Recently, a H-NOX domain of chemotaxis

receptor was discovered in a thermophilic anaerobe *Thermoanaerobacter tengcongensis*.[22] This protein is termed *Tt* H-NOX. Unlike H-NOX domains from eukaryotes (sGC) and facultative aerobes that do not bind O_2, *Tt* H-NOX has been shown to have tight O_2 ligand affinity.[22]

Thermoanaerobacter tengcongensis (Tt) H-NOX

Compared with Hb and Mb, *Tt* H-NOX has several advantages for therapeutic oxygen delivery. For example, *Tt* H-NOX display better thermal stability, as its oxygen bound complex has been confirmed stable at temperatures from 0 ºC to 80 ºC, the higher of which is the physiologically relevant temperature of its native organism.[23] Also, WT *Tt* H-NOX and its mutants were revealed to have low NO reactivity. The NO dioxygenation rate (the reaction rate of the ferrous-oxy protein with NO) for WT *Tt* H-NOX was determined as 0.051 $\mu M^{-1}s^{-1}$, which is the slowest reported for globins.[24] The I75F, L144F, and I75F/L144F mutants were reported to have NO dioxygenation rates of 0.19 $\mu M^{-1}s^{-1}$, 0.64 $\mu M^{-1}s^{-1}$ and 2.0 $\mu M^{-1}s^{-1}$, respectively. All of these rates are among the slowest reported.[24] In addition, the lack of autoxidation, the resistance to denaturation and the extremely long-term stability have all made *Tt* H-NOX a promising candidate for therapeutic oxygen carrier development.[23, 25]

However, with an oxygen dissociation constant determined as 89.7 nM, WT *Tt* H-NOX binds O_2 too tightly for therapeutic applications.[23] As a result, it would not be comparable as Hb to supply O_2 for tissues. To solve this problem, scientists have been investigating the modulation of ligand affinity of *Tt* H-NOX since the crystal structure was solved in 2004.[22] Several residues within the heme pocket such as Y140, L144 and

H102 were found to contribute to controlling oxygen affinity, and site directed mutagenesis was performed at these sites (Figure 2).[23, 19a, 26, 24b]

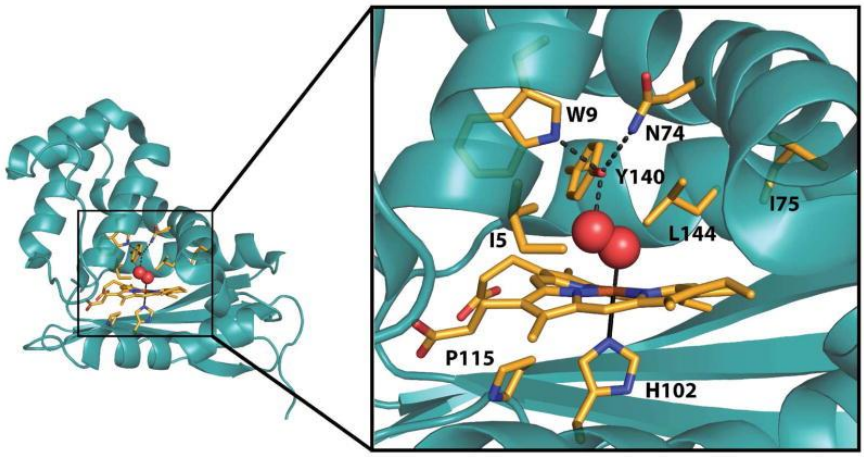

Figure 2: Key residues and the heme within the *Tt* H-NOX heme pocket
Reprinted with permission from Reference 26. Copyright (2011) American Chemical Society.

Tt H-NOX	K_d O_2 (nM)	k_{off} O_2 (s^{-1})	k_{on} O_2 (μM^{-1} s^{-1})
WT	89.7	1.2	13.6
W9F	305	1.84	6.02
Y140L	~1400	20.1	N/A
W9F/Y140L	N/A	N/A	N/A
I75F	497	11.19	22.5
L144F	2360	16.06	6.8
I75F/L144F	11150	45.7	4.1
I5F	1570	61.3	39.0

Table 1: Kinetics constant of *Tt* H-NOX mutants[23, 26, 24b]

The most distinguishing feature of *Tt* H-NOX is the distal hydrogen bond network: Y140 forms a stable hydrogen bond with the bound oxygen, while W9 and N74 form hydrogen bonds with Y140 to stabilize the hydrogen bond network.[23] When tyrosine 140 is mutated to leucine (Y140L), the oxygen affinity decreases substantially (K_d from 89.7 nM to 1400 nM). Mutation of both Y140 and W9 results in the double mutant W9F/Y140L, which completely loses oxygen binding capability.[23]

Distal pocket bulk also plays a critical role in modulating the oxygen affinity of *Tt* H-NOX: upon introduction of bulky phenylalanine residue to position I75 or L144, which are both located in the distal pocket, k_{off} increases 9-fold and 13-fold respectively.[24b] These two positions have synergistic effect on oxygen affinity, as it has been shown that the double mutant I75F/L144F has a 37-fold increase of k_{off} value. This is due to the addition of distal pocket bulkiness leading to a more open structure and affecting the proximal histidine orientation.[24b]

The proximal histidine H102, which forms an iron-histidine bond with the heme, is able to rotate around the iron-histidine bond and can exhibit two major configurations: staggered and eclipsed (Figure 3). As previously predicted by computational work and confirmed by experimental results, the oxygen affinity of *Tt* H-NOX varies based on different configurations, due to tuning the Fe-O_2 bond strength.[27, 24b]

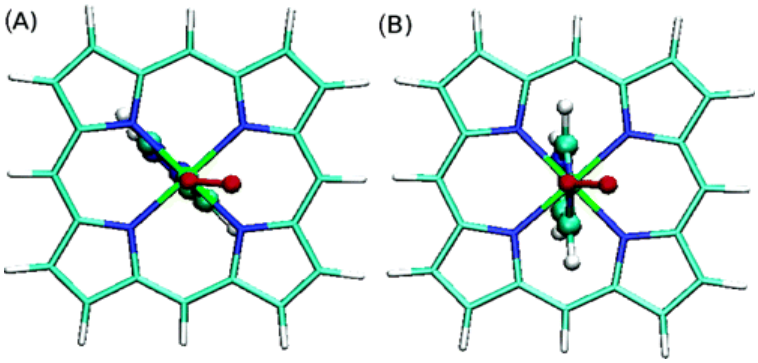

Figure 3: Proximal histidine rotational position: (A) eclipsed and (B) staggered
Reprinted with permission from Reference 27. Copyright (2006) American Chemical Society.

Other conserved residues around the heme pocket such as I5 and P115 also modulate the oxygen affinity. The mutation of I5F increases O_2 association rates 1.56 fold and dissociation rates 50 fold as compared to WT *Tt* H-NOX, through alternating the flexibility of protein conformation.[26] When the P115A mutation is introduced, the heme

cofactor adopts a flattened conformation. The decreased heme distortion leading to an increased oxygen affinity by decreasing the redox potential of the heme iron.[19a] These results show a clear link between the heme conformation, protein structure and *Tt* H-NOX properties.

In summary, *Tt* H-NOX is amenable to mutagenesis and its oxygen affinity can be modulated. By using sited directed mutagenesis, several important residues and mutants have been discovered and characterized. It was found that the distal effects determine the oxygen binding capability of *Tt* H-NOX to a large extent, in combination with proximal effects. Specifically, a variety of factors such as hydrogen bond, bulkiness and configuration are operating this capability cooperatively.

However, the oxygen binding affinity of *Tt* H-NOX mutants is still much tighter than natural Hb and does not reach the optimal range for therapeutic applications (K_d = 20-30 μM). But since *Tt* H-NOX proteins display superior physiological properties than Hb such as high thermal stability, low NO reactivity, lack of autoxidation and excellent long-term stability, it is considered as a highly promising candidate for artificial oxygen carrier, while its oxygen binding affinity requires further engineering.

A major challenge that needs to be overcome is the previously used time intensive structure guided rational design. For example, previous research has been limited on generating mutations within the heme pocket of *Tt* H-NOX due to the difficulty to make prediction beyond heme pocket. Additionally, conducting mutagenesis site by site is not feasible given the time required. Therefore, in order to utilize the advantages of *Tt* H-NOX to address the worldwide blood shortage problem, an effective and efficient method for engineering mutants with optimal oxygen affinity is in need.

In this study, we address the limitations of past approaches and describe a novel method for engineering heme proteins as potential blood substitutes. The general experimental design is illustrated in Figure 4. Directed evolution techniques are used to evolve libraries of *Tt* H-NOX heme proteins that can be screened for useful properties for therapeutic oxygen delivery. In general, the screening cycle consists of three procedures: the initial high throughput screen refines the library to contain only cells that express heme-bound proteins, while other cells are discarded. Then, the calibrated optical based medium throughput screen assays are performed to identify the *Tt* H-NOX mutants with desired oxygen affinity. Heme proteins with binding affinity outside of the optimal range (K_d = 20-30 μM) are discarded. Following identification of desired mutants, comprehensive characterization is necessary to further investigate other useful properties of the mutants such as stability and biocompatibility. Their compatibility and suitability for the usage of blood substitute will be further engineered and optimized.

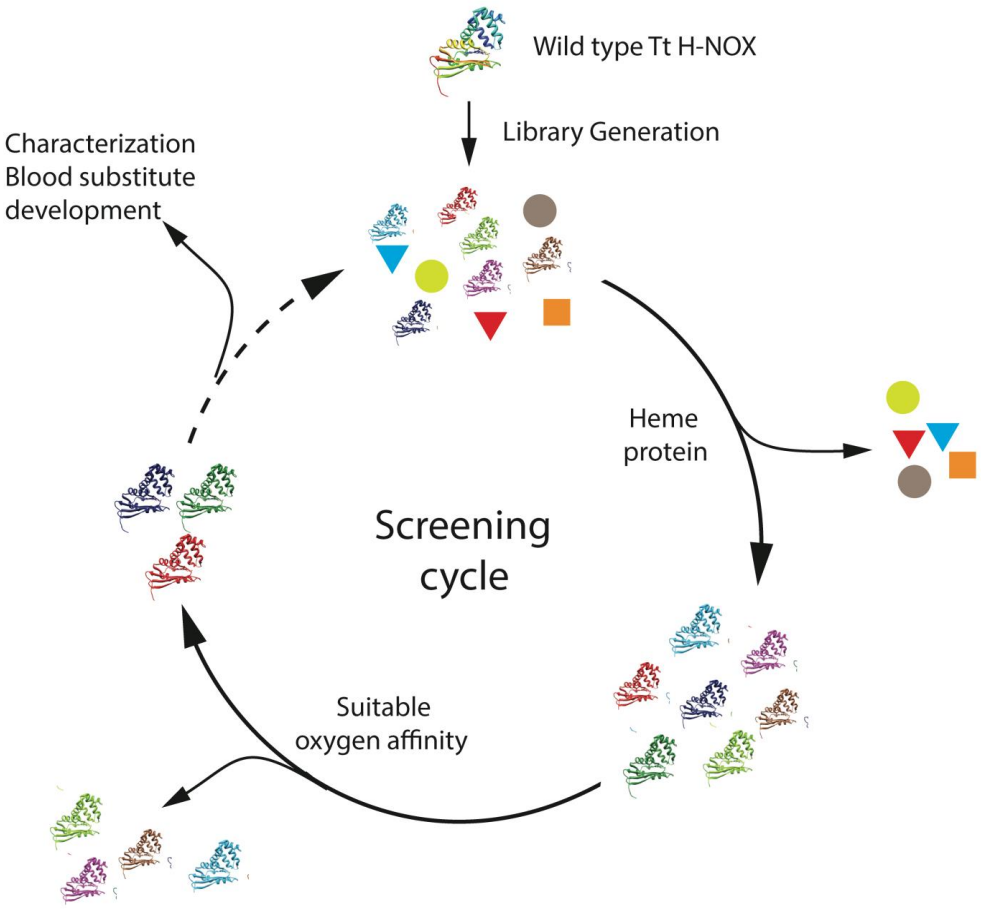

Figure 4: General scheme of experimental design

In our experiments, site saturation mutagenesis was used to generate a mutant library at sites with preliminary interest (Y140, L144, G71 and G143). A blue fluorescent protein based high throughput heme incorporation screen was developed as the initial screen, which identified heme-bound proteins in whole cells. In addition, a luciferase-based bioluminescence assay and a HRP-based fluorescence assay were developed as oxygen affinity screen. By correlating the oxygen dissociation constant of the protein with the luminescence or fluorescence output, the protein's oxygen affinity was optically measured in 96-well plates.

Results and Discussion

Tt H-NOX Protein Characterization

Wild type (WT) *Tt* H-NOX and its mutants were expressed and purified following the optimized protocol as described in the Methods section. The ferrous-unligated, ferrous-oxy, ferrous-CO, ferrous-NO, ferric-unligated, and ferric-CN states were generated, characterized and compared to previously published data.[28] Each ligation state has a characteristic UV-Vis spectrum- a Soret band from 390-435 nm and α/β bands around 550-600 nm.[28] Detection and differentiation of the ligation states by UV-Vis spectroscopy demonstrated that the purified proteins are heme-bound. Figure 5 shows a typical UV-Vis absorption spectrum of WT *Tt* H-NOX. The ferrous-unligated *Tt* H-NOX has a Soret band at 431 nm, while the ferrous-oxy *Tt* H-NOX forms a Soret band at 417 nm and split α/β bands in the 550-600 nm range, indicating O_2 is bound.

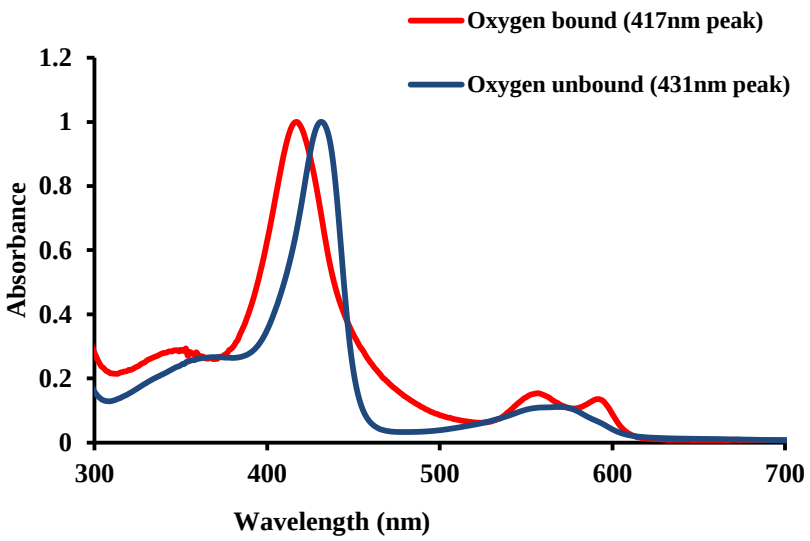

Figure 5: UV-Vis spectra of ferrous-unligated and ferrous-oxy WT *Tt* H-NOX

Site Saturation Library Generation

Several residues of *Tt* H-NOX such as Y140 and L144 have previously been investigated, and the site directed mutagenesis experiments have been proved to dramatically change the oxygen affinity of *Tt* H-NOX.[23, 24b] However, even though it is clear that each of these residues plays an important role in modulating oxygen affinity, the exact effect of substitution with all the other possible amino acids is unknown. Therefore, site saturation mutagenesis (SSM) was used to generate a comprehensive library, containing all natural amino acids at set positions including Y140, L144, G71 and G143. SSM has been considered as an efficient method to generate small DNA libraries with high protein diversity at single sites and achieve directed evolution.[29] It is hypothesized that the results will be able to further explain the mechanism of how those residues modulate the general oxygen affinity of *Tt* H-NOX.

As discussed in the introduction, Y140 in the distal pocket of *Tt* H-NOX directs hydrogen bonds to bound oxygen molecules and contributes significantly to the oxygen affinity.[22] Additionally, upon the addition of distal pocket bulkiness to L144, the oxygen affinity decreases substantially due to a more open structure formed (Figure 2).[24b] Thus, by saturating Y140 and L144 sites, it is expected to uncover how different amino acids would alter the ligand affinity.

It was revealed that G70 and G144 serve as a pivotal point in SO2144 H-NOX, a *Tt* H-NOX homolog found in *Shewanella oneidensis*.[30] These two glycines are both located outside heme pocket, but they are conserved throughout the H-NOX family.[30] The corresponding residues in *Tt* H-NOX are G71 and G143 respectively. Thus, G71 and

G143 were chosen for SSM and were expected to become a starting point for us to explore ligand affinity regulation beyond the active site of *Tt* H-NOX.

The site saturation library was evolved using modified methods of site directed mutagenesis.[31] Instead of introducing different amino acid codons for each mutant, primer sets containing a degenerate mixture of the four bases were used. It was previously reported by Zheng *et al.* that if the primers were not completely overlapping, higher mutations rates would be achieved.[32] However, when both primer sets were designed and tested with WT *Tt* H-NOX templates, it was found that completely overlapping primers worked more effectively than partially overlapping ones for our experiments. With few exceptions, the generated library was collections of recombinant clones that contain all 20 naturally occurring amino acids at the specific sites of interest.

SSM is time efficient and cost effective that can potentially be utilized in high throughput directed evolution. It was found that a single amino acid substitution is sufficient to obtain a necessary level of protein performance enhancement.[29] However, it is possible that to attain optimal oxygen affinity of *Tt* H-NOX proteins, further combinations of mutations or generations of randomized libraries will be necessary.

Development of High Throughput Heme Incorporation Assay

As the generated library is likely to result in non-heme binding mutants as well as heme-bound proteins, non-functional proteins need to be removed from the library before screening for O_2 affinity. To determine if heme is bound to the generated protein mutants, a sensitive assay is needed. Arnold *et al.* have reported a heme incorporation screen assay that based on absorption peak shift due to CO molecule binding.[33] By using carbon

monoxide difference spectroscopy, the absorption peak of functioning cytochrome P450 was observed to red-shift to 450 nm, which gave a sensitive indicator of heme incorporation and proper folding of P450 proteins.[33] However, this method requires protein mutants to be extracted from *E. coli* cells before measurements; otherwise the absorption signal would be buried in the whole cell background. In our experiments, in order to screen a randomly established mutant library in the future, it is advantageous to develop an initial high throughput method to selectively distinguish heme incorporation in single cell level without protein purification.

The heme group is a chromophore that can strongly absorb light from 416 to 431 nm, depending on the oxidation/ligation state of the iron. It was found that the absorbance spectrum overlaps with the emission spectrum of many blue-green fluorophores such as blue fluorescent protein (Figure 6). Therefore, we hypothesized that if heme could work as an efficient quencher that absorbs the fluorescence emitted by a nearby fluorophore in the cell, then the presence of heme proteins in cells should be able to be determined based on fluorescence intensity. If a fluorophore containing cell were expressing a heme-free *Tt* H-NOX mutant, the fluorescence signal of the fluorophore would remain at a normal level; otherwise, heme proteins in the cell would decrease the fluorescence signal.

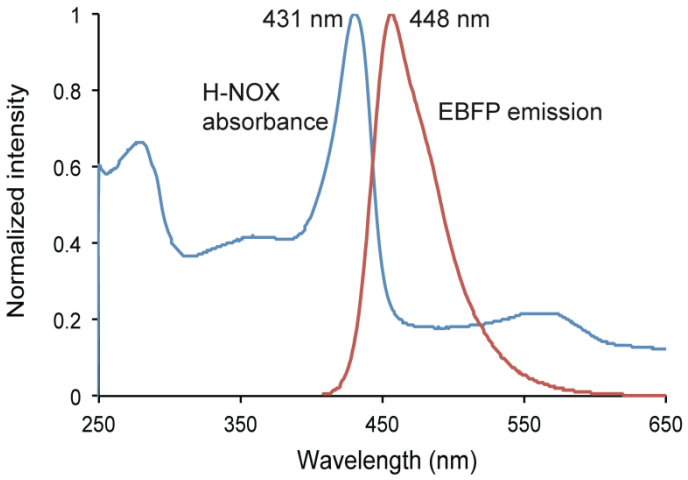

Figure 6: Overlap of *Tt* H-NOX absorbance and BFP emission spectra

The variant of *Aequorea* green fluorescent protein (GFP) known as blue fluorescent protein (BFP) was originally engineered by substituting histidine 66 for tyrosine in the chromophore precursor sequence.[34] An improved version of BFP has been shown to have higher brightness and photostability.[35] BFP has a maximum excitation wavelength at ~385 nm, and emission wavelength at ~450 nm, which has a good overlap with the heme absorbance wavelength of *Tt* H-NOX (Figure 6). Therefore, it was used as the fluorophore to pair with the quencher heme.

In this procedure, BFP and *Tt* H-NOX are co-expressed in *E. coli* cells. In cytoplasm, due to energy level overlapping, the fluorescence of excited BFP can be quenched by *Tt* H-NOX through dynamic quenching (Figure 7). In addition, the fluorescence emitted by BFP can be reabsorbed by heme proteins. Therefore, due to this dual-mechanism, the fluorescence of BFP should be effectively lowered in heme proteins expressed cells compared to their counterparts.

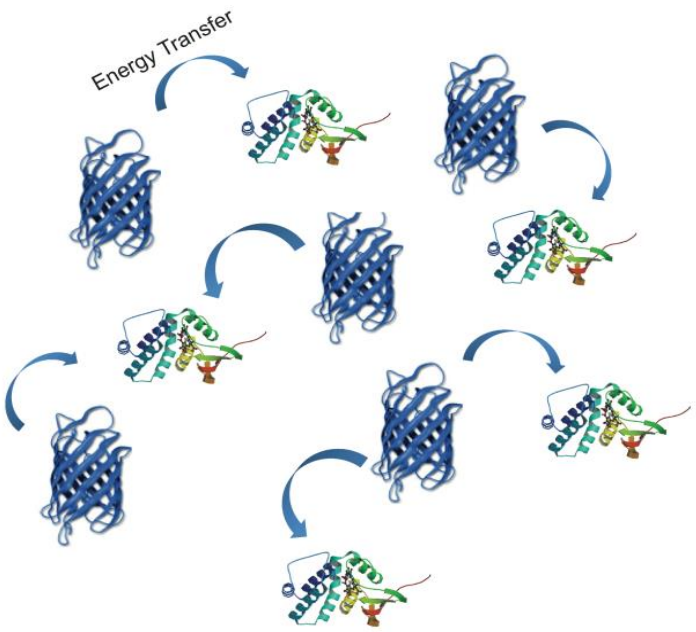

Figure 7: Scheme of dynamic quenching of fluorescence by heme (PDB ID of WT *Tt* H-NOX: 1U56; BFP: 1BFP)

The BFP gene (Addgene) was purchased in a pBAD vector with ampicillin resistance. Because *Tt* H-NOX is usually expressed from a pET20b vector, which also has ampicillin resistance, changing the antibiotic resistance of one of these two genes was required for co-expression. Thus, the resistance marker of BFP plasmid was switched from ampicillin to kanamycin using one-step sequence- and ligation-independent cloning (SLIC).[36] The cloning results were confirmed by gel and sequencing. A detailed procedure can be found in the Methods section.

In addition, H102G and a *Tt* H-NOX truncated at the residue M98 were obtained through site directed mutagenesis. These two mutants do not contain the conserved H102 residue, which is located in the proximal heme pocket and binds heme. Thus, both H102G and truncated *Tt* H-NOX should have little or no heme bound, respectively. As a result, they were used as controls for the heme-based fluorescence quenching experiment.

To test this quenching model, BFP and *Tt* H-NOX were co-expressed using Tuner (DE3) PlysS cells. After expression, cells were diluted to the same OD 600 level before conducting fluorescence measurements. BFP fluorescence was excited at 385 nm, and emission spectra were scanned from 400 to 520 nm. As seen in Figure 8, when BFP was the only protein expressed, very high fluorescence intensity was observed. However, when BFP was co-expressed with WT *Tt* H-NOX, the fluorescence emission was significantly lower, which could be due to dynamic quenching of heme. The fluorescence of co-expression samples of BFP with H102G or with truncated *Tt* H-NOX was greater as compared with WT *Tt* H-NOX. This can be explained as significantly less heme were bound in these control samples, resulting in less quenching. Assuming that the *Tt* H-NOX truncation did not quench fluorescence but did modulate protein expression yields, the quenching efficiency of WT *Tt* H-NOX is calculated as 31.5%.

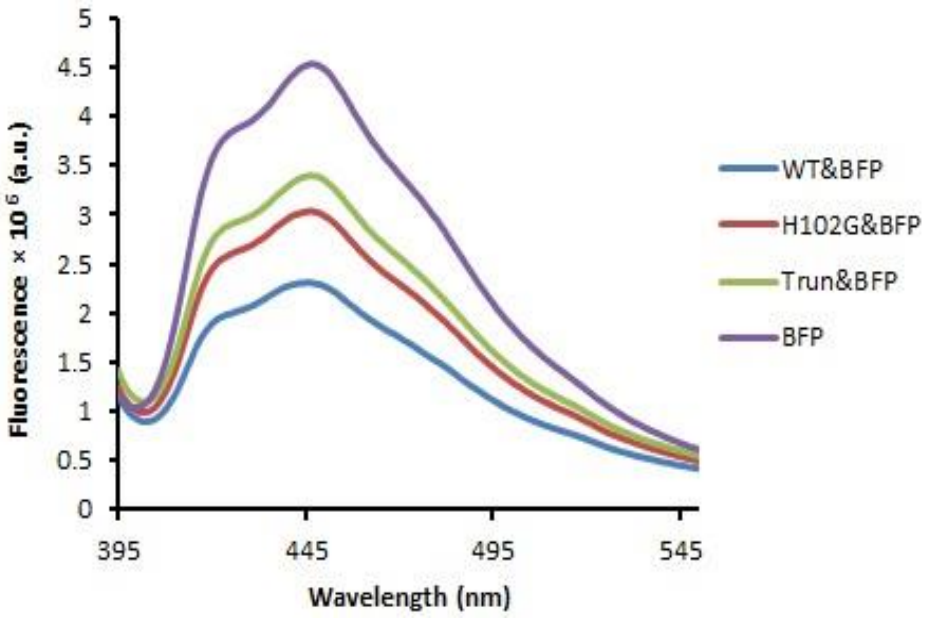

Figure 8: Fluorescence emission spectra of quenching experiment

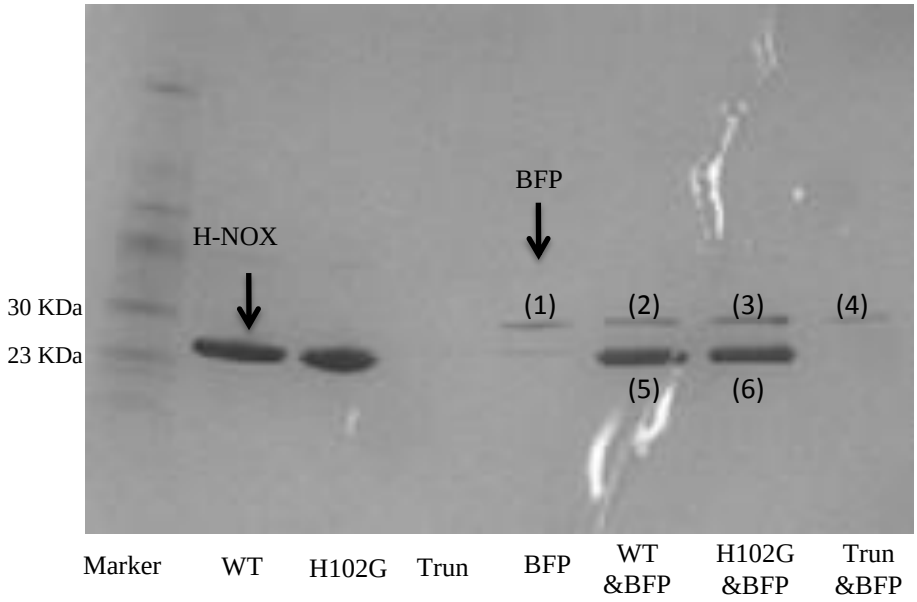

Figure 9: SDS PAGE gel of co-expression samples

To confirm co-expression, cells were lysed within BugBuster (Novagen). Because both proteins have hexa-histidine tag, they were purified by cobalt resin. The purified samples were then analyzed by SDS PAGE. As shown in Figure 9, when only WT or H102G *Tt* H-NOX was expressed, a single band was shown with a mass of ~23 KDa, corresponding to the mass of *Tt* H-NOX. When truncated *Tt* H-NOX was expressed, no band was shown since the mutant had no hexa-histidine tag to bind the resin. When BFP was expressed alone, only one band was found at molecular weight of ~27 KDa, which corresponds to the predicted molecular weight of BFP. However, when BFP was co-expressed with *Tt* H-NOX (WT or H102G), two bands were shown, indicating expressed BFP and expressed *Tt* H-NOX respectively.

To quantify the expression level, the gel image was analyzed by ImageJ. The data of protein content is shown in Table 2. The BFP expression levels in the co-expression samples of WT and H102G *Tt* H-NOX were much higher than that of truncated *Tt* H-NOX. However, the BFP fluorescence intensity was the highest for the truncated *Tt* H-NOX, indicating heme-quenching fluorescence in WT and H102G *Tt* H-NOX. Therefore, the BFP/heme-based quenching method was validated and supported by this preliminary protein expression analysis. In the future, the analysis of a large scale of cells with different expression levels is required to investigate the effect of protein expression fluctuation on this dynamic quenching behavior.

Protein	(1)	(2)	(3)	(4)	(5)	(6)
Protein content (a.u.)	3885	6095	9714	2925	19699	19534

Table 2: Protein contents analysis

Based on different fluorescence level for each mutant containing cell, fluorescence-activated cell sorting (FACS) can subsequently be employed to identify and isolate desired host cells with the expected fluorescence intensity, which will be served as the initial screen of the generated library.[37] The threshold will be set for heme-unbound protein since the original fluorescence intensity should be high without quenching, and any signal below such intensity will be treated as potential heme-bound cells, and will be collected for further identification and screening.

Since this BFP/heme-based quenching method is a negative screen, which would possibly be affected by other factors, a positive screen will be needed to confirm heme incorporation in the selected cells. Any cells that pass the FACS after several rounds of

selection will be subjected to a second screen with absorption measurement. The protein mutants will be extracted from cells and then measured by UV-Vis spectroscopy. A characteristic peak of Soret band is a confirmation that heme-bound proteins are present in the selected cell.

Development of Oxygen Affinity Screening Assay

Once heme-bound protein containing cells are isolated, the next step is to screen for *Tt* H-NOX mutants with optimal oxygen binding affinity (K_d = 20-30 μM). There are several sophisticated methods such as laser flash photolysis that can be used to characterize the oxygen association constant, and stopped flow techniques that can characterize the oxygen dissociation constant, as previously described for heme proteins kinetics measurements.[23, 24b] However, most of the current methods are low throughput and measure oxygen binding of one type of protein at a time, making it very challenging to conduct a large scale screening from random libraries. To overcome this limitation, multiple optical based oxygen affinity screening assays including luciferase-based luminescence assay and HRP-based fluorescence assay, were developed and compared in this study.

In general, oxygen-bound *Tt* H-NOX mutants are added to a plate in anaerobic environment. Following equilibration, the amount of oxygen released by each mutant is measured by the assays, and converted to optical output. To achieve higher throughput detection, 96-well plates are used and the optical signal is measured by a plate reader. The values should be directly correlated with the amount of oxygen released by each *Tt*

H-NOX and provide an end-point measurement of the oxygen dissociation constant of each mutant.

Luciferase Assay

Luciferase mediated luminescence is one of the most well-known examples of bioluminescence process. Commercial luciferase assay kits have been widely used in detecting the concentration of ATP and as reporter molecule for gene expression.[38] In the presence of ATP, Mg^{2+} and O_2, light is produced by exploiting the chemical energy of luciferin oxidation, forming the final product molecule oxyluciferin, which generates luminescence at the wavelength of ~550 nm (Figure 10).[39] Therefore, we hypothesized that with an excess of luciferin, ATP and Mg^{2+}, the luminescence intensity should be proportional to oxygen concentration in the reaction system. By measuring luminescence in 96-well plate format, this method can provide a quick strategy to quantify dissolved oxygen.

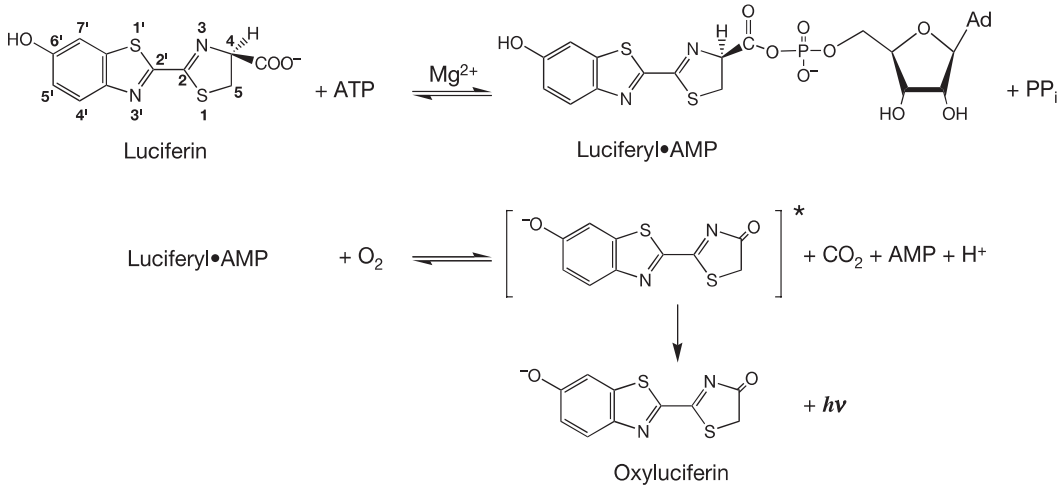

Figure 10: Luciferase-based bioluminescence reaction[40]

Reprinted by permission from Macmillan Publishers Ltd: [Nature] Reference 40, Copyright (2006)

Because the goal of the assay is to detect trace amounts of oxygen released from proteins, developing a high quality isolation from ambient oxygen turns as the priority. Usually, sample preparation could be performed in anaerobic chamber, while the measurement was conducted in aerobic environment. Thus, to prevent outside oxygen from interfering with the anaerobic reaction system, several kinds of oil including silicon oil and mineral oil were degassed and tested. However, it was found in our preliminary study that external oxygen was still diffusing into the solution with a layer of oil over the solution. According to Arain *et al.*, PET sealer and aluminum foil would be better choices to seal the plate, although oil can decrease the oxygen diffusion speed.[41] In this study, since the output signal needs to be detected on top of the wells, aluminum foil could not be applied to our setup. Thus, transparent PET sealer was chosen as the top cover above a layer of mineral oil (Figure 11).

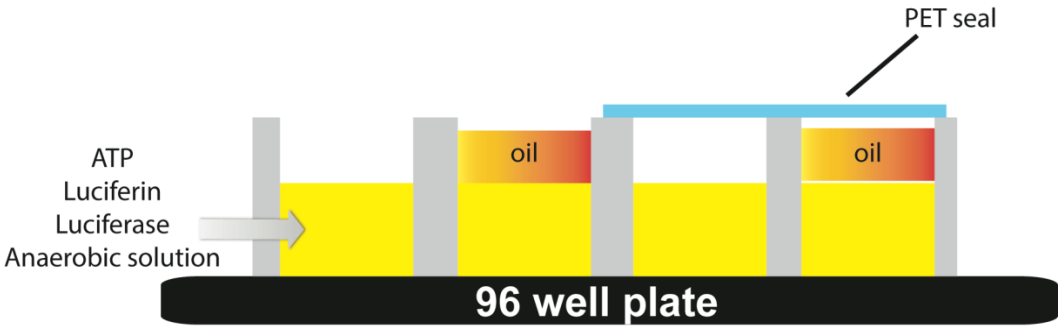

Figure 11: Scheme of anaerobic experimental setup design

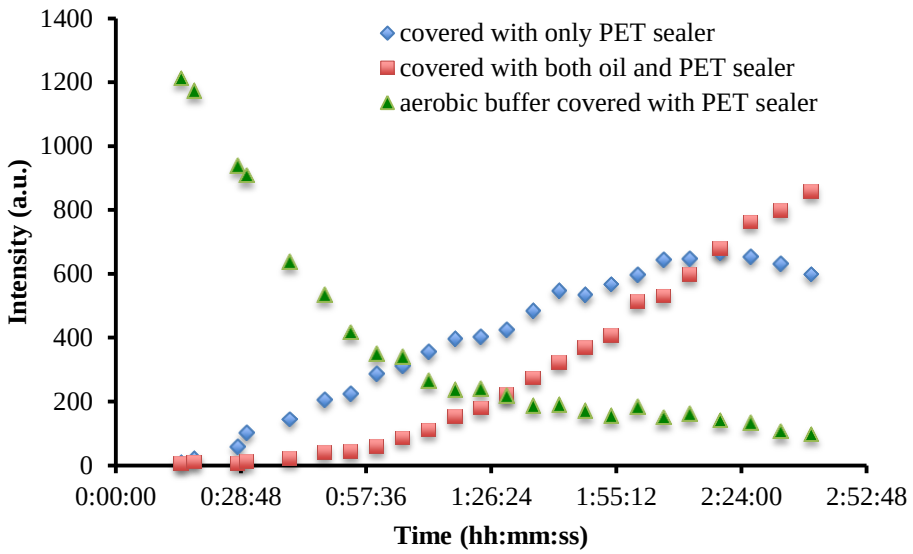

Figure 12: Real time monitoring of oxygen in experimental setup

To test the sealing quality of the setup, the luminescence intensity as a function of time was plotted and compared between different cases (Figure 12). All the materials were prepared in anaerobic chamber to ensure no oxygen contamination. Then the experiment was conducted in anaerobic chamber and measured on a plate reader in aerobic environment. When anaerobic solution was covered with PET sealer, minimum oxygen diffused into the plate in the first 30 min, which was a big improvement compared with mineral oil alone as the cover, where oxygen would diffuse in immediately. More significantly, when both mineral oil and PET sealer were applied, much less oxygen diffused into the solution based on the low level of luminescence detected in the first 60 min. The results indicate that the high sealing efficiency provided by this setup can exclude most interference from outside oxygen in future experiments. In the control experiment, when aerobic solution was used instead of anaerobic solution, the luminescence intensity was very high in the beginning of the reaction, indicating high

concentration of dissolved oxygen. Then the signal decreased gradually due to luminescence decay.

To measure the oxygen concentration of an unknown solution, it is necessary to first establish a calibration curve showing the luminescence intensity as a function of oxygen concentration. According to literature, at room temperature, aerobic water contains 256 μM dissolved oxygen.[42] Thus, by mixing different ratios of aerobic and anaerobic luciferin reagent (containing Mg^{2+} and ATP), different oxygen concentrations could be achieved. Upon the addition of anaerobic luciferase and with each well fully sealed, the luminescence signal was measured immediately. As shown in Figure 13, the luciferase activity is correlated with the amount of oxygen added, displaying a linear curve in a dynamic range from 0 to 250 μM.

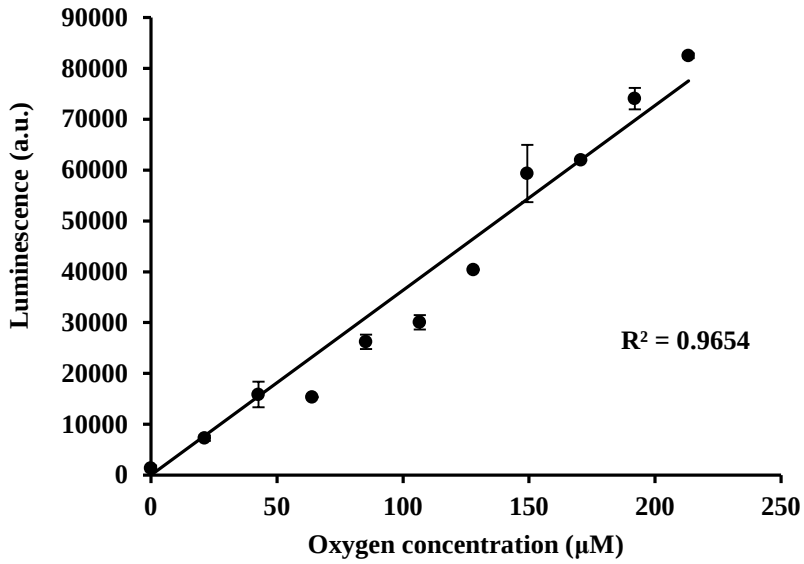

Figure 13：Calibration curve of luminescence vs. oxygen concentration in the range of 0-250 μM

However, this oxygen concentration range is not applicable for K_d measurement since natural heme proteins usually release smaller amount of oxygen based on

estimations with known dissociation constant values as well as our experiment settings. To make the measurement more accurate, a narrower oxygen range was used (0 to 60 μM), and a similar linear relationship was obtained (Figure 14).

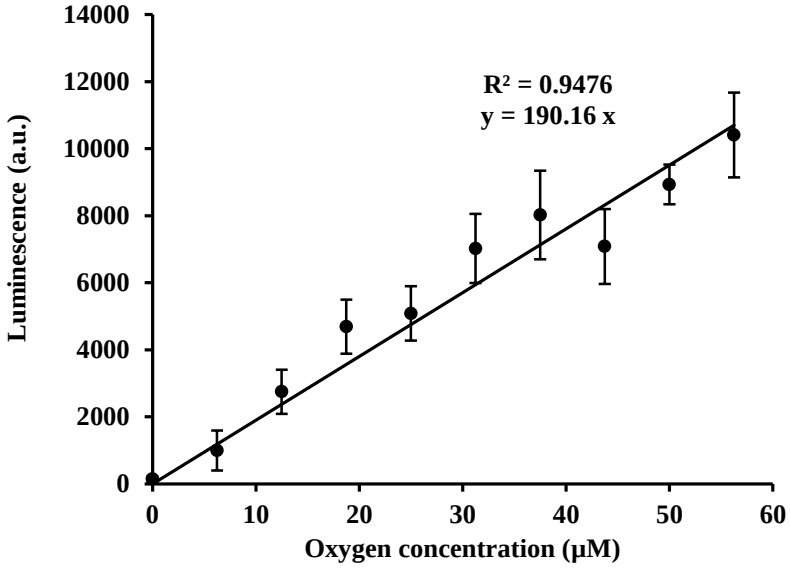

Figure 14：Calibration curve of luminescence vs. oxygen concentration in the range of 0-60 μM

To determine the oxygen dissociation constant of protein mutants, the luminescence intensity of each protein sample needs to be measured and converted using the calibration curve. Our preliminary study confirmed that the luminescence of oxylucinferin would not be quenched by heme absorbance. Then a novel medium throughput design was developed, as illustrated in Figure 15.

Tt H-NOX proteins were reduced to the ferrous state and then saturated with oxygen. The concentration of the proteins was determined spectrophotometrically by measuring the absorbance at 416-417 nm. It was reported that the extinction coefficient of the ferrous-oxy Soret band is 89,000 $\mu M^{-1}cm^{-1}$.[28] After mixing with Ni-NTA modified magnetic beads in aerobic environment, these his-tagged proteins were fully bound to the

beads, allowing the aerobic supernatant to be removed. Then the protein bound beads were brought into anaerobic chamber and incubated with anaerobic luciferin reagent, enabling oxygen to release from the proteins to the solution.

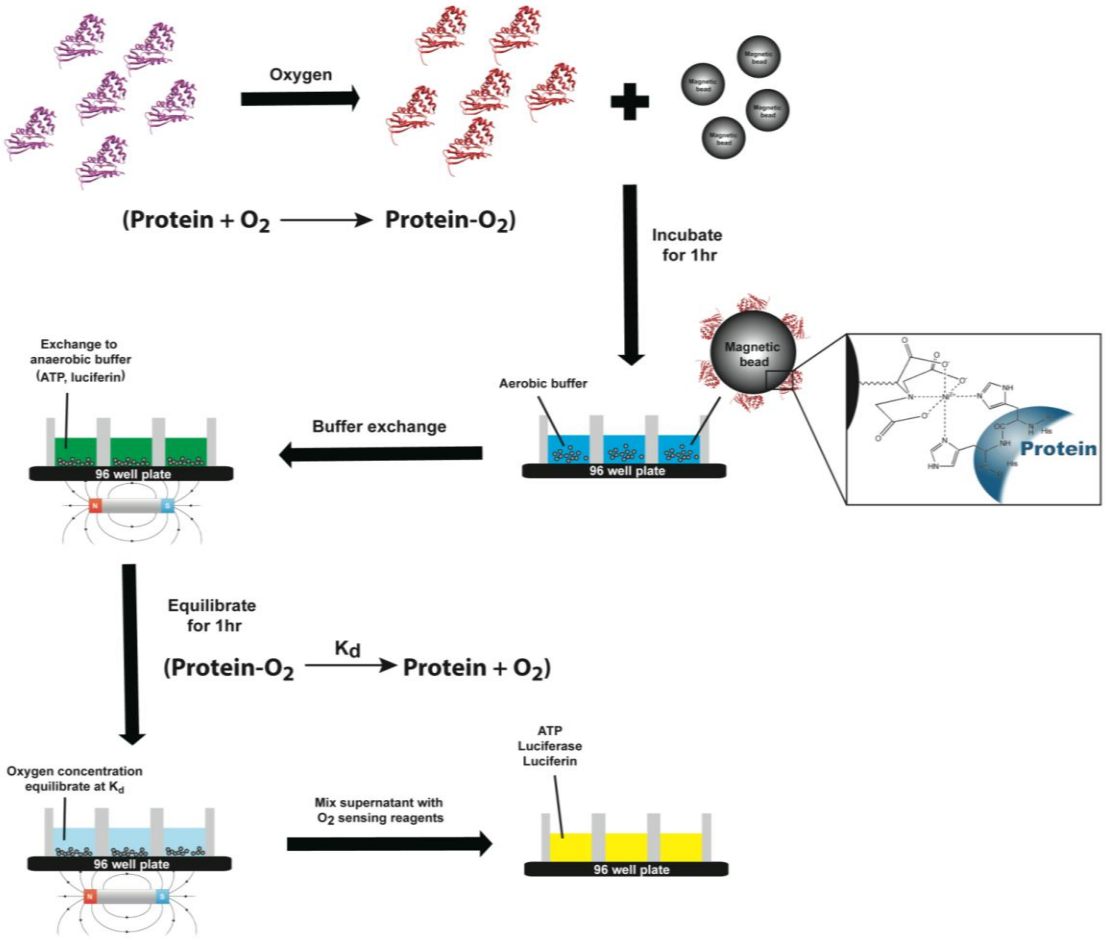

Figure 15: General scheme of experimental procedure of protein K_d measurement

After one-hour incubation, the system was expected to have reached its equilibrium, since protein-ligand interaction can usually reach its equilibrium within $4.6/k_{off}$ seconds.[43] In the case of heme-oxygen interaction, the k_{off} can range widely from 0.01 to 1000 s^{-1},[44] leading to the value of $4.6/k_{off}$ from below 0.01 s to 4600 s. Thus, the one-hour incubation time should be sufficient for most of the heme proteins to reach equilibrium with anaerobic solution, except for proteins with extremely high affinity.

Therefore, during the incubation, a certain amount of oxygen was released into the anaerobic luciferin reagent based on the oxygen dissociation constant of the proteins. Finally, the oxygen dissolved luciferin reagent was transferred into an anaerobic 96-well plate containing luciferase. Upon the initiation of the reaction, the luminescence signal was measured immediately. By generating a correlation between luminescence output, oxygen concentration and protein dissociation constant, a calibrated oxygen affinity assay was expected to be developed.

To quantify the feasibility of the experimental design, theoretical calculation models were performed. In equilibrium, the dissociation constant is defined as [Protein][O_2]/[Protein-O_2]. Because only oxygen-bound proteins (concentration determined by UV-Vis spectroscopy) were added into each well initially, the concentration of unbound protein and free oxygen always had the same values. In addition, based on the linear oxygen titration curve shown in Figure 14, the luminescence intensity is proportional to the concentration of oxygen (Equation 1), with which the value of [O_2] as well as [Protein] was determined by the luminescence intensity. In the equilibrium process, at first, 50 nmol of oxygen-bound proteins were added in 220 µL of buffer solution. Assuming during incubation, x nmol of oxygen had been released by the oxygen-bound proteins, the value of x can be related to oxygen concentration by Equation 2. Finally, by integrating equation 1 and 2 with the dissociation constant calculation, the value of K_d is related to the concentration of oxygen in the solution as well as the luminescence intensity (Equation 3). Thus, luminescence versus oxygen concentration (Figure 14) can be converted to the new plot showing luminescence versus K_d (Figure 16).

Equation 1: $\text{Luminescence(a.u.)} = 190.16 \times [O_2](\mu M)$

Equation 2: $x(\text{nmol}) = [O_2] \times V = [O_2](\mu M) \times 220(\mu L) \times 10^{-3}$

Equation 3: $K_d = \frac{[O_2] \times [\text{Protein}]}{[\text{Protein} - O_2]} = \frac{\frac{x}{V} \times \frac{x}{V}}{\frac{50 - x}{V}} = \frac{x^2}{(50 - x) \times V} = \frac{x^2 \times 10^3}{(50 - x) \times 220} (\mu M)$

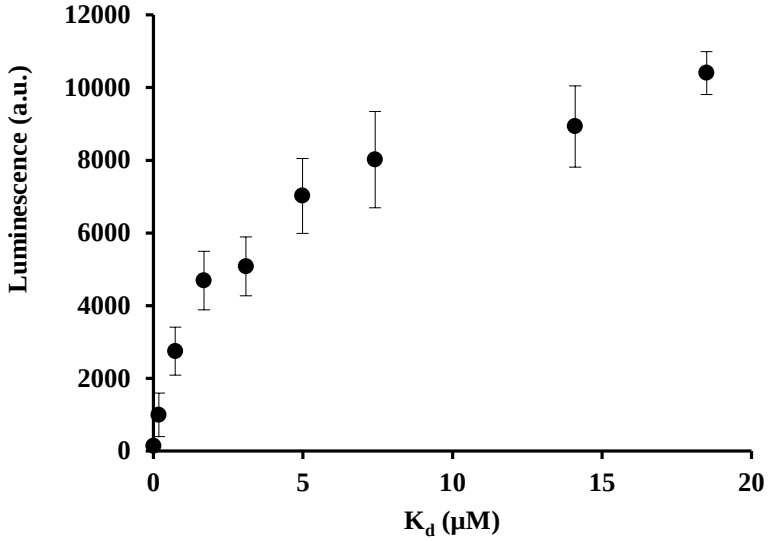

Figure 16: Theoretical curve of luminescence vs. K_d of proteins

To calibrate the oxygen titration curve and the theoretical luminescence versus K_d curve, WT *Tt* H-NOX and several mutants with known K_d values were expressed, purified and tested using the described procedure (Figure 15). In Table 3, the reported dissociation constants of WT, L144F and I75F/L144F *Tt* H-NOX are shown, with the experimental luminescence values and corresponding calculated K_d values. The protein data displayed are the average of triplicated measurements. The data imply that the assay still has a large and different oxygen background level from batch to batch, possibly due to the existence of residual oxygen after incubation in anaerobic chamber.

	Experimental Intensity	Experimental K_d (μM)	Reported K_d (μM)
WT	~7100	~7.3	0.0897
L144F	~14617	~42.5	2.360
I75F/L144F	~15305	~44.1	11.15

Table 3: Luciferase assay with known *Tt* H-NOX proteins

HRP Assay

Due to difficulties with developing a luciferase assay, a horseradish peroxidase (HRP) reaction cycle was used to develop the oxygen affinity assay. In the presence of oxygen, glucose can be converted to gluconolactone by glucose oxidase, which also generates hydrogen peroxide (H_2O_2) in the reaction. The H_2O_2 will then be used by a coupled reaction, where HRP will oxidize its substrate Amplex Red into a red fluorescent product, resorufin, in a 1:1 stoichiometry. In the meantime, oxygen will be generated as a product of this reaction and participate as one of the reactants in the first step of the reaction cycle.[45]

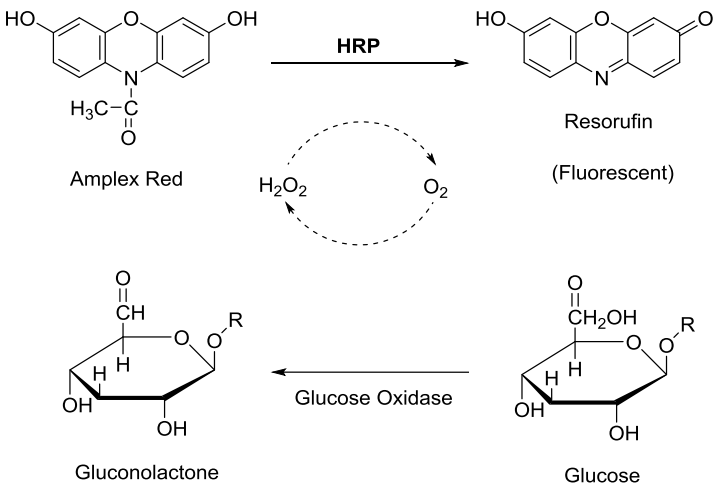

Figure 17: HRP-based fluorescence reaction

Given its high sensitivity, specificity, and chemical stability, the HRP reaction cycle has been widely used in detection of glucose, oxidases and H_2O_2 inside and outside of cells.[46] Resorufin has fluorescence excitation and emission maxima of approximately 570 nm and 585 nm, which greatly minimize interference of the autofluorescence in most biological samples. In our preliminary study, it was also confirmed that at these wavelengths, the fluorescence was not quenched by heme absorbance.

The experimental design is consisted of an excess of HRP, Amplex Red, glucose and glucose oxidase, with a limiting amount of oxygen, which should result in the fluorescence output being directly correlated with oxygen concentration. Since this reaction cycle uses oxygen as reactant as well as product, the resulting fluorescence signal should be amplified. In addition, all the components of this assay were purchased as powder instead of liquid reagents, dissolved into buffer in an anaerobic chamber, and used when fresh to minimize interference of external oxygen. The HRP assay had the potential to be more sensitive and reliable than luciferase assay, since HRP assay can amplify the useful signal with lower background oxygen.

Similar to the luciferase assay, a calibration curve between fluorescence output and oxygen concentration was established. To achieve this, different oxygen concentrations were obtained by mixing aerobic and anaerobic solutions at different ratios. After addition of all reagents into wells, 96-well plates were covered with previously described sealing covers. Particularly, the aluminum foil cover was necessary before measurement to prevent oxygen penetration from ambient environment and photo-oxidation of Amplex Red. After 10 min incubation at room temperature, the fluorescence

intensity of all samples was measured on a plate reader, with an excitation wavelength at 530 nm, and a detection wavelength at 590 nm.

To find out the optimal range for the calibration curve, three sets of oxygen concentration ranges were tested for this HRP assay. In Figure 18-20, the fluorescence intensity was plotted as a function of oxygen concentration. The intensity is linear at the low concentration range of the curves, indicating a high correlation between oxygen concentration and fluorescence. Interestingly, after the oxygen concentration increased towards 100 μM, the fluorescence output increased very slowly and eventually reached a plateau (Figure 18). This observation was consistent with previous findings that extremely high levels of glucose or glucose oxidase can produce lower fluorescence than moderately high levels, since excess of H_2O_2 resulting from the reaction of glucose with glucose oxidase can convert the reaction product, resorufin, to nonfluorescent resazurin.[47] Therefore, it was possible that high oxygen involved in the reaction shown in Figure 18 could have also resulted in excess H_2O_2, which oxidized resorufin into the nonfluorescent byproduct resazurin.

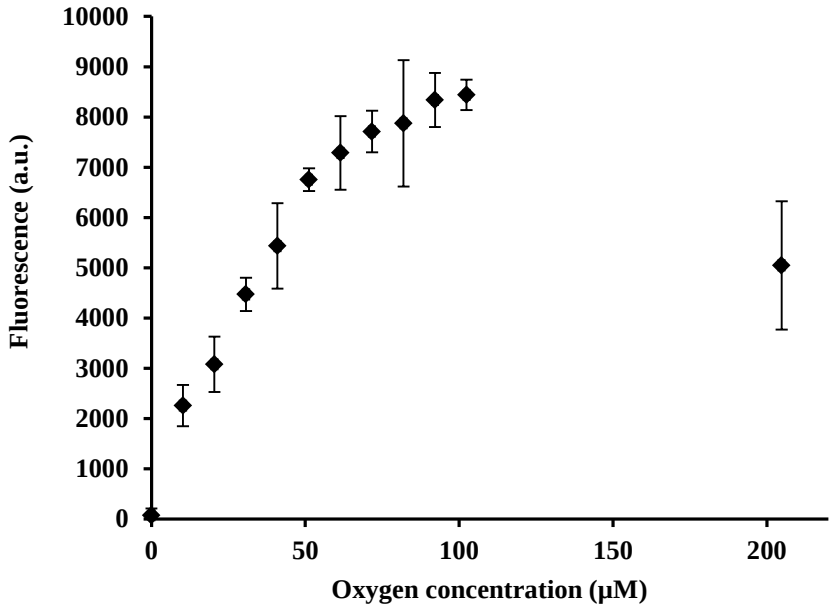

Figure 18: Calibration curve of fluorescence vs. oxygen concentration in the range of 0-200 μM

In order to exclude the high H_2O_2 interference, a lower oxygen concentration range (0 - 56 μM) was tested. In Figure 19, fluorescence output increased proportionally to oxygen concentration and no plateau was observed, suggesting this calibration curve is applicable for HRP assay. In addition, since it was speculated that HRP assay could be extremely sensitive in the very low oxygen range, an even lower range with more data points was obtained in Figure 20. The linearity of the curve is very high (0-28 μM), with a similar slope value in Figure 19. These calibration curves prove the HRP assay with high confidence.

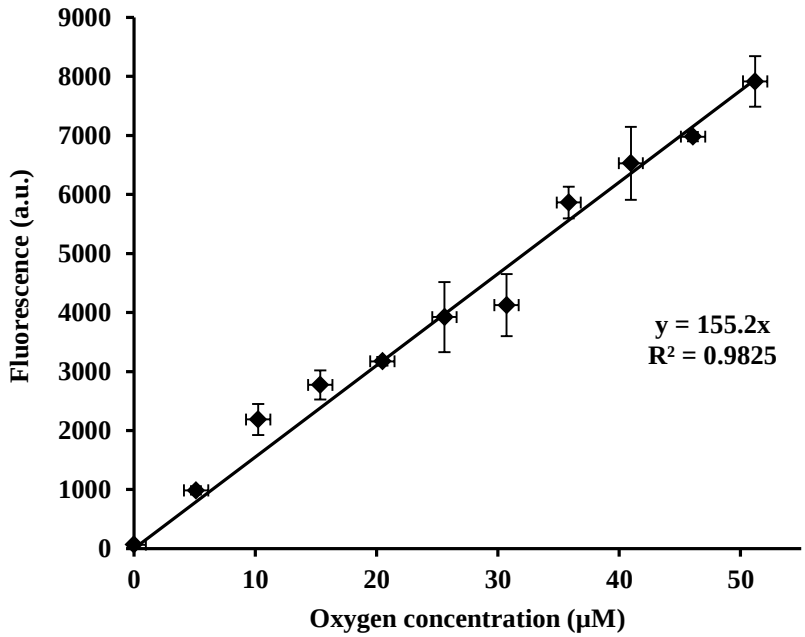

Figure 19: Calibration curve of fluorescence vs. oxygen concentration in the range of 0-56 µM

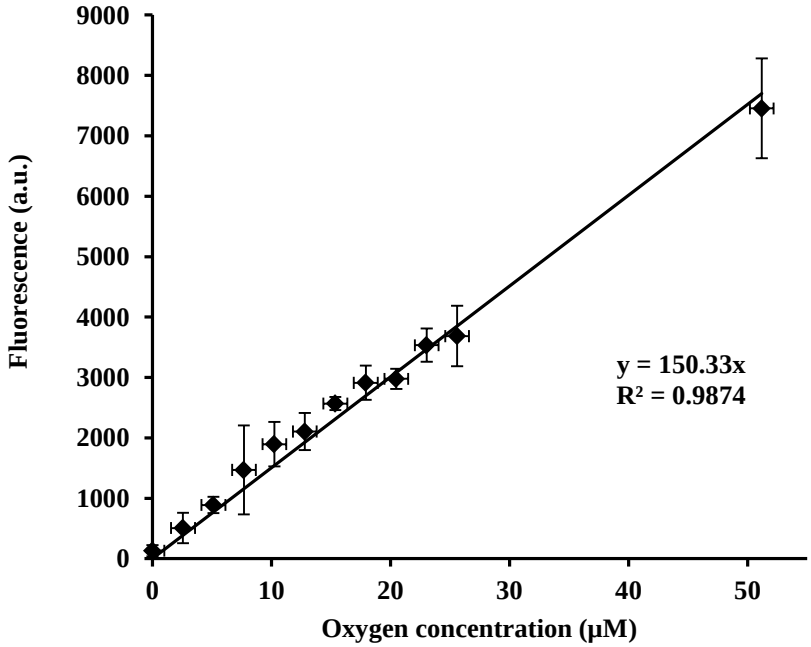

Figure 20: Calibration curve of fluorescence vs. oxygen concentration in the range of 0-28 µM

Since the fluorescence intensity in the HRP assay is cumulative, the readout value is highly related to initial oxygen concentration and reaction time. At various time points, the signal readout would be different due to a combination of fluorescence accumulation and decay. At a fixed reaction time, the initial concentration of oxygen released from proteins would also affect the intensity value. Therefore, to simulate the dependence of protein concentration on final intensity, three concentrations of the same protein type (50μM, 100μM, and 200 μM) were assumed to generate light with the essay after 10 min fixed reaction time. By fitting the data to equations similar to the luciferase assay (Equation 1-3), different curves were generated (Figure 21). According to this theoretical model, with the addition of higher amount of proteins, it should be easier to achieve higher intensity value with the same K_d due to more oxygen release.

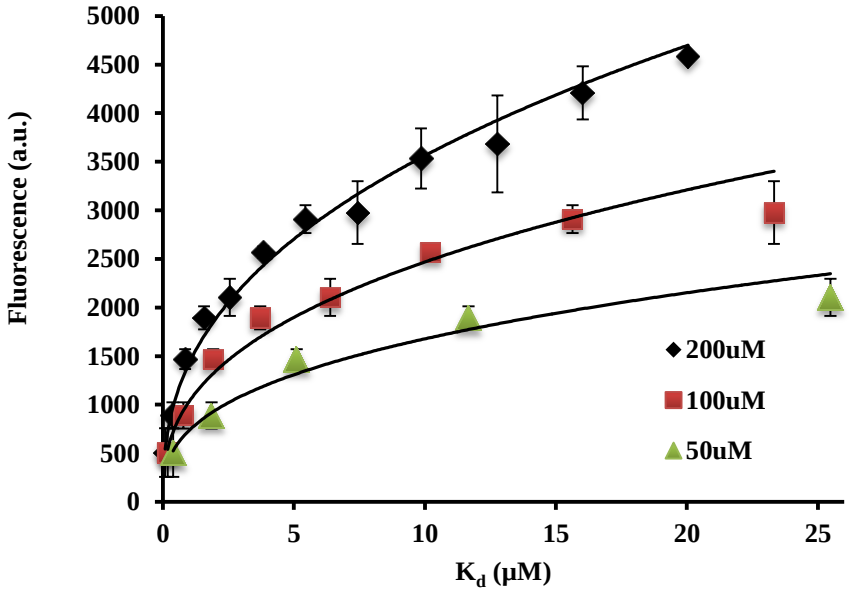

Figure 21: Theoretical curve of fluorescence vs. K_d of proteins

With the calculated fluorescence versus K_d plot, *Tt* H-NOX proteins with known K_d values were used to test the HRP assay. The procedure was previously illustrated in Figure 15. Briefly, protein mutants in their ferrous-oxy state were bound to Ni-NTA modified magnetic beads, and were allowed to equilibrate in anaerobic working solution containing Amplex Red, HRP and glucose oxidase. Assuming the solution had reached its equilibrium after 30 min incubation, it was transferred to an anaerobic 96-well plate containing glucose. The glucose oxidase used the O_2 released from *Tt* H-NOX to generate H_2O_2, which was subsequently used by HRP to oxidize Amplex red into fluorescent resorufin. The fluorescence was measured on a plate reader, and the intensity of each well should be directly correlated with the O_2 released by each *Tt* H-NOX mutant.

	Experimental Intensity	Experimental K_d (μM)	Reported K_d (μM)
L144F (50 μM)	~2752	~39.7	2.360
L144F (200 μM)	~3659	~12.6	2.360
I75F/L144F (50 μM)	~6117	~366.6	11.15
I75F/L144F (200 μM)	~5920	~35.8	11.15

Table 4: HRP assay with known *Tt* H-NOX proteins

Therefore, an end-point measurement of the O_2 dissociation constant of each protein was achieved by calculating according to the theoretical model (Figure 21). As shown in Table 4, based on the intensity analysis with 200 μM protein addition, the experimental K_d of L144F and I75F/L144F is calculated as ~12.6 μM and ~35.8 μM, while the actual dissociation constant of L144F and I75F/L144F has been reported as 2.36 μM and 11.15 μM, respectively.[24b] These differences are in a reasonable range

considering multiple steps existed during sample preparation. Also, these values are much more acceptable when compared with another set of data acquired with the addition of 50 μM protein. This comparison further suggests that higher concentration of proteins is preferred for the HRP assay, which should lead to more reliable results and minimize the effect of experiment errors.

Conclusion and Future Directions

Given the worldwide blood shortage situation, ongoing research is necessary to develop an alternative supply of healthy blood with optimal oxygen binding affinity. While studies have mainly focused on engineering Hb and Mb into artificial therapeutic oxygen carriers,[5, 12] this study investigates a class of heme sensor proteins, *Tt* H-NOX, due to its available structural information, tunable oxygen affinity and extraordinary stability. Instead of modulating the oxygen affinity of *Tt* H-NOX by site directed mutagenesis, directed evolution techniques such as site saturation mutagenesis were used. A SSM library of *Tt* H-NOX was evolved at the sites of preliminary interests (Y140, L144, G71 and G143). With the advantage of low DNA redundancy and high protein diversity, the SSM library generation was efficient and can be used for screen. In order to screen functional heme-bound proteins from the SSM or other random libraries in the future, a high throughput BFP-based heme incorporation screen was developed and tested. Because the BFP emission spectrum has a fairly large overlap with the heme absorbance spectrum of *Tt* H-NOX, it was shown that BFP fluorescence could be quenched by heme when co-expressed in *E. coli*. Therefore, by judging the fluorescence level of co-expression samples, the production of heme-bound *Tt* H-NOX can be determined in *E. coli*. Once heme containing proteins are identified and isolated, a luciferase-based bioluminescence assay and a HRP-based fluorescence assay were developed to test the oxygen binding affinity of the proteins. By correlating the oxygen dissociation constant of *Tt* H-NOX with the luminescence or fluorescence output, proteins' oxygen affinity was optically measured in 96-well plates. Although both assays are theoretically reliable, the HRP assay showed much higher reproducibility and simplicity, due to the lack of

oxygen in sample preparation. The HRP assay was utilized to measure the K_d of several *Tt* H-NOX proteins with known dissociation constants. The results showed discrepancy between our measured values and reported values. To future optimize the assay, higher concentration of proteins is recommended, which can minimize the effect of ambient oxygen interference during the whole process. Eventually, these screening assays can be applied onto the SSM and random libraries in the future to screen *Tt* H-NOX with optimal oxygen affinity. In all, these studies will also highlight residues outside the heme active site that are important for modulating ligand binding affinity, and make a contribution to the discovery of future artificial blood substitutes.

Experimental Methods

Site Directed Mutagenesis

Site directed mutant I75F was created with mutagenic primers:

FP: 5’ – GGTAGGAAGGCAGAACTTTAAAACTTTCAGCGAATG – 3’

RP: 5’ – CATTCGCTGAAAGTTTTAAAGTTCTGCCTTCCTACC – 3’

Double mutant I75F/L144F was created using I75F mutant as template, and with mutagenic primers:

FP: 5’ – GATTACTTTTTAGGGTTTATAGAGGGTAGTTC – 3’

RP: 5’ – GAACTACCCTCTATAAACCCTAAAAAGTAATC – 3’

H102G mutant was created with mutagenic primers:

FP: 5’ – GATGATGGATGAGGTAGGCCTACAGCTTACCAAG – 3’

RP: 5’ – CTTGGTAAGCTGTAGGCCTACCTCATCCATCATC – 3’

Truncated *Tt* H-NOX mutant was created by introducing a stop codon at the site M98 (before H102). Mutagenic primers used:

FP: 5’ – GTGAATTTTTTAATGATGTAAGATGAGGTACACCTACAG – 3’

RP: 5’ – CTGTAGGTGTACCTCATCTTACATCATTAAAAAATTCAC – 3’

PCR was performed using *Phusion* polymerase (New England Biolabs) and run according to manufacturers’ conditions. *Dpn*I (New England Biolabs) was added to 4% of the total volume and incubated for 2 hours at 37 ºC. PCR solutions were immediately transformed into DH5α (New England Biolabs).

Tt H-NOX Expression

Expression and purification of *Tt* H-NOX were performed as previously described, with minor modification.[24b] Cultures were grown at 37 ºC until OD 600 reaches 0.6-1.0 (45 g bacto-yeast extract, 1.6 g KH_2PO_4, 11.5 g of $K_2HPO_4 \cdot 3H_2O$, 15 mL glycerol). After cooled to 20 ºC, the cultures were induced with 500 µM 5-aminolevulinic acid (OChem, Inc.), 10 µM isopropyl-β-D-thiogalactopyranoside (Research Products International Corp.). The cultures were incubated at 20 ºC for 18-20 hours, and then were harvested by centrifugation at 6,000 rpm for 15 min. The pellets were stored at -80 ºC.

Tt H-NOX Purification

Pellets were thawed on ice with low imidazole buffer (50 mM TEA buffer, 300 mM NaCl, 10 mM imidazole, 5% glycerol, pH 7.4), 1 mM pefablock (GoldBio, tech), and 0.015 mg/mL DNaseI (Calbiochem). The solution was mixed until homogeneous and lysed using a homogenizer (EmulsiFlex-C5). The lysates were heat-denatured at 70 °C for 30 min and then centrifuged at 37,000 rpm for 60 min. The supernatant was loaded onto a cobalt column previously equilibrated with low imidazole buffer. The proteins were washed with 25 column volumes of low imidazole buffer and eluted with 5 column volumes of high imidazole buffer (50 mM TEA, 300 mM NaCl, 150 mM imidazole, 5% glycerol, pH 7.4). After the proteins were concentrated, they were desalted with a PD 10 column (GE Healthcare) into storage buffer (50 mM TEA, 20 mM NaCl, 5% glycerol, pH 7.4). If the proteins were not adequately purified with solely a cobalt column, they were subjected to a gel filtration column (GE Healthcare; HiLoad 26/600) by FPLC (Bio-Rad; BioLogic Duo Flow). The proteins were then

concentrated, aliquoted, and immediately frozen in liquid nitrogen, and stored at -80 ºC. An example of SDS PAGE gel of purified WT *Tt* H-NOX is shown in Figure 22.

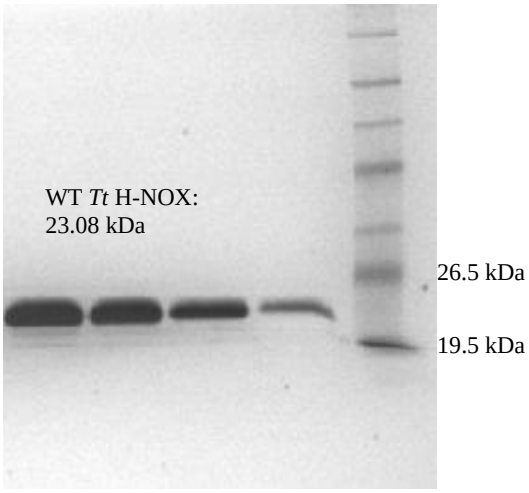

Figure 22: An example of SDS PAGE gel of purified WT *Tt* H-NOX

Absorption Spectra

Absorption spectra were obtained in storage buffer (50 mM TEA, 20 mM NaCl, 5% glycerol, pH 7.4). *Tt* H-NOX was oxidized to its ferric state by adding excess potassium hexacyanoferrate(III) (Sigma-Aldrich). The ferric-CN spectrum was detected upon the addition of cyanide reagent. The ferrous-unligated state was formed with the addition of excess sodium dithionite (Acros Organics). By exposing ferrous-unligated heme to aerobic buffer, ferrous-oxy state was produced. By purging CO gas into ferrous-unligated heme, ferrous-CO state was produced. With the addition of NONOate, ferrous-NO state was produced. Ligand binding was observed by UV-Visible spectroscopy (Cary 100 UV-Vis spectrometer).

Site Saturation Mutagenesis Library Generation

SSM library was created with primer sets containing a degenerate mixture of the four bases in the mutagenic region. Below is an example of SSM primers for L144 site:

FP1: 5' – GATTACTTTTTAGGGNHTATAGAGGGTAGTTC – 3'

RP1: 5' – GAACTACCCTCTATADNCCCTAAAAAGTAATC – 3'

FP2: 5' – GATTACTTTTTAGGGBGTATAGAGGGTAGTTC – 3'

RP2: 5' – GAACTACCCTCTATACVCCCTAAAAAGTAATC – 3'

FP3: 5' – -GATTACTTTTTAGGGTGGATAGAGGGTAGTTC – 3'

RP3: 5' – GAACTACCCTCTATCCACCCTAAAAAGTAATC – 3'

FP4: 5' – GATTACTTTTTAGGGVAGATAGAGGGTAGTTC – 3'

RP4: 5' – GAACTACCCTCTATCTBCCCTAAAAAGTAATC – 3'

FP5: 5' – GATTACTTTTTAGGGATGATAGAGGGTAGTTC – 3'

RP5: 5' – GAACTACCCTCTATCATCCCTAAAAAGTAATC – 3'

The degenerate primers were mixed according to the ratio of the corresponding codons. PCR was performed using *Phusion* polymerase and run according to manufacturers' conditions. *Dpn*I was added to 4% of the total volume and incubated for 2 hours at 37 ºC. PCR solutions were immediately transformed into DH5α.

SLIC Cloning

The BFP gene (Addgene) was purchased in a pBAD vector and the resistance marker was switched from ampicillin to kanamycin using one-step sequence- and ligation-independent cloning (SLIC).[36]

Primers used:

FP: 5’ – TTCTCAGAATGACTTGGTTGAGTGTGTAGGCTGGAGCTGCTTC – 3’

RP: 5’ – ATGCTTTTCTGTGACTGGTGAGTCATATGAATATCCTCCTTAG – 3’

pBAD vector was digested with *Sca*I overnight, and the linearized vector was purified with a PCR purification kit (Promega). After purification, the linearized vector and kanamycin insert were mixed at a 1:2 molar ratio. 0.2 µL of T4 DNA polymerase (3 U/ µL, NEB) was added to the mixture and incubated at room temperature for 2.5 min. The reaction was stopped immediately by putting the mixture on ice. After incubating on ice for 10 min, the SLIC solution was transformed into DH5α. The cloning results were confirmed by sequencing.

Co-expression of *Tt* H-NOX and BFP

Tt H-NOX and BFP gene was transformed into Tuner (DE3) pLysS cells with 100 µg/mL Ampicillin, 40 µg/mL kanamycin and 30 µg/mL chloramphenicol. Single colonies were selected to make overnight cultures with correct antibiotics. 1 mL of this overnight culture was added to 10 mL LB culture with correct antibiotics. Cultures were grown at 37 ºC until OD 600 reaches 0.6-1.0. After cooled to 20 ºC, the cultures were then induced by 10 µM Isopropyl β-D-1-thiogalactopyranoside, 20% arabinose, and 500 µM aminolevulinic acid. After induction, cultures were grown at 20 ºC overnight. Cultures were then harvested by centrifugation at 10,000 g for 10 min and stored at -80 ºC.

Purification of BFP/*Tt* H-NOX Co-expression Samples

The small-scale expression was lysed within BugBuster (Novagen). Cell pellets were frozen prior to resuspension in BugBuster (0.5 mL per 10 mL culture was added). 1 µL (25 units) Benzonase Nuclease per 1 mL BugBuster reagent was used for resuspension. The cell suspension was incubated on a shaking platform at a slow setting for 10–20 min at room temperature. The extract was not viscous at the end of the incubation. By centrifugation at 16,000 × g for 20 min at 4 °C, the insoluble cell debris was removed. The soluble extract was loaded directly onto a cobalt resin previously equilibrated with 10 column volumes of low imidazole buffer. The protein was washed with 10 column volumes of low imidazole buffer and eluted with 5 column volumes of high imidazole buffer. The purified proteins were stored at -80 ºC.

Luciferase Assay - Oxygen Titration

Serial dilutions were performed on firefly luciferase (Promega) with 1 mg/mL BSA, and stored at -80 ºC. Luciferin (Promega) was ordered as pre-mixed liquid reagent containing ATP and Mg^{2+}, and stored at -80 ºC. Prior to use, luciferase and luciferin was thawed on ice. After degassing by gently purging with helium gas for an hour, anaerobic luciferase and luciferin were produced and brought into anaerobic chamber. Different ratios of aerobic and anaerobic luciferin reagent were mixed to provide different oxygen concentrations. A total volume of 100 µL of luciferin reagent was added into 20 µL of luciferase to initiate the reaction, and 100 µL mineral oil and PET sealer was applied as sealing cover. Luminescence was measured by a plate reader (Biotech), with a sensitivity of 70.

Luciferase Assay - *Tt* H-NOX Oxygen Affinity Measurement

Tt H-NOX proteins were reduced to the ferrous state by adding sodium dithionite in anaerobic chamber, and the ferrous-oxy *Tt* H-NOX was produced by exposing to oxygen saturated buffer. An anaerobic plate was taken out of the anaerobic chamber. 400 µL Ni-NTA modified magnetic beads slurry was added into wells. Oxygen bound protein was added after the removal of beads slurry buffer. After incubation for 30 min, all of the supernatant was taken to measure UV-Vis spectra. By comparing the original protein concentration and the supernatant concentration, the amount of protein bound to the beads was calculated. The plate was sealed with PET sealer and taken into anaerobic chamber, and 120 µL of anaerobic luciferin reagent was added into each well. After incubation for 60 min, 100 µL of this equilibrated solution was transferred into another anaerobic plate containing 20 µL of luciferase in each well. Upon the initiation of the reaction, the plate was covered with 100 µL mineral oil and PET sealer. Luminescence was detected immediately on a plate reader with a sensitivity of 70. A set of oxygen titration was performed on the same plate as reference.

HRP Assay - Oxygen Titration

10 mM Amplex red stock solution (Invitrogen) was prepared with anaerobic DMSO. 10 U/mL HRP (Sigma-Aldrich) stock solution, 100 U/mL glucose oxidase (Sigma-Aldrich) stock solution and 400 mM glucose stock solution were prepared with anaerobic 1X buffer (0.05 M sodium phosphate, pH 7.4). An anaerobic working solution containing 100 µL HRP stock solution, 100 µL glucose oxidase stock solution, 50 µL Amplex Red stock solution and 750 µL 1X buffer was prepared subsequently. Different ratios of

aerobic and anaerobic 1X buffer were mixed to provide different oxygen concentrations. A total volume of 80 µL 1X buffer was added into 10 µL glucose solution and 10 µL working solution. 100 µL mineral oil, PET sealer and aluminum foil were applied as sealing cover. After incubation at room temperature for 10 min, fluorescence was measured by a plate reader with an excitation wavelength of 530 nm, detection wavelength of 590 nm. The set sensitivity was 50.

HRP Assay - *Tt* H-NOX Oxygen Affinity Measurement

Tt H-NOX proteins were reduced to the ferrous state by adding sodium dithionite in anaerobic chamber, and the ferrous-oxy *Tt* H-NOX was produced by exposing to oxygen saturated buffer. An anaerobic plate was taken out of the anaerobic chamber. 80 µL beads slurry was added into wells. Oxygen bound protein was added after the removal of beads slurry buffer. After incubation for 30 min, all of the supernatant was taken to measure UV-Vis spectra. By comparing the original protein concentration and the supernatant concentration, the amount of protein bound to the beads was calculated. The plate was sealed with PET sealer and taken into anaerobic chamber. 100 µL anaerobic 1X buffer was added into each well. After incubation for 30 min, 80 µL of the solution was transferred into another plate containing 10 µL glucose and 10 µL working solution in each well. Upon the initiation of the reaction, the plate was covered with 100 µL mineral oil, PET sealer and aluminum foil. After incubation at room temperature for 10 min, fluorescence was detected on a plate reader with a sensitivity of 50. A set of oxygen titration was performed on the same plate as reference.

References

1. (a) Scott, M. G.; Kucik, D. F.; Goodnough, L. T.; Monk, T. G., Blood substitutes: evolution and future applications. *Clin. Chem.* **1997,** *43* (9), 1724-1731; (b) Simon, T. L., Where have all the donors gone? A personal reflection on the crisis in America's volunteer blood program. *Transfusion* **2003,** *43* (2), 273-279.

2. Busch, M. P.; Kleinman, S. H.; Nemo, G. J., Current and emerging infectious risks of blood transfusions. *JAMA, J. Am. Med. Assoc.* **2003,** *289* (8), 959-962.

3. Organization, W. H., Global database on blood safety. *Summary Report* **2001,** *2002*.

4. Riess, J. G., Oxygen Carriers ("Blood Substitutes") Raison d'Etre, Chemistry, and Some Physiology. *Chem. Rev.* **2001,** *101* (9), 2797-2920.

5. Alayash, A. I., Hemoglobin-based blood substitutes: oxygen carriers, pressor agents, or oxidants? *Nat. Biotechnol.* **1999,** *17* (6), 545-549.

6. Honig, C. R., Modern cardiovascular physiology. **1988**.

7. Rossi-Fanelli, A.; Antonini, E., Studies on the oxygen and carbon monoxide equilibria of human myoglobin. *Arch. Biochem. Biophys.* **1958,** *77* (2), 478-492.

8. Mayfield, J. A.; Dehner, C. A.; DuBois, J. L., Recent advances in bacterial heme protein biochemistry. *Curr. Opin. Chem. Biol.* **2011,** *15* (2), 260-266.

9. Ghosh, A., CO, NO, and O2 as vibrational probes of heme protein active sites. *The Smallest Biomolecules: Diatomics and their Interactions with Heme Proteins. Elsevier* **2011**.

10. (a) Roberts, G. P.; Kerby, R. L.; Youn, H.; Conrad, M., CooA, a paradigm for gas sensing regulatory proteins. *J. Inorg. Biochem.* **2005,** *99* (1), 280-292; (b) Stone, J. R.; Marletta, M. A., Soluble guanylate cyclase from bovine lung: activation with nitric oxide and carbon monoxide and spectral characterization of the ferrous and ferric states. *Biochemistry* **1994,** *33* (18), 5636-5640.

11. Voet, D.; Voet, J. G., Hemoglobin. *Biochemistry, John Wiley & Sons* **2004,** *1*, 591.

12. Dou, Y.; Maillett, D. H.; Eich, R. F.; Olson, J. S., Myoglobin as a model system for designing heme protein based blood substitutes. *Biophys. Chem.* **2002,** *98* (1), 127-148.

13. Azarov, I.; Huang, K. T.; Basu, S.; Gladwin, M. T.; Hogg, N.; Kim-Shapiro, D. B., Nitric oxide scavenging by red blood cells as a function of hematocrit and oxygenation. *J. Biol. Chem.* **2005,** *280* (47), 39024-39032.

14. Doherty, D. H.; Doyle, M. P.; Curry, S. R.; Vali, R. J.; Fattor, T. J.; Olson, J. S.; Lemon, D. D., Rate of reaction with nitric oxide determines the hypertensive effect of cell-free hemoglobin. *Nat. Biotechnol.* **1998,** *16* (7), 672-676.

15. Moisan, S.; Drapeau, G.; Burhop, K. E.; Rioux, F., Mechanism of the acute pressor effect and bradycardia elicited by diaspirin crosslinked hemoglobin in anesthetized rats. *Can. J. Physiol. Pharmacol.* **1998,** *76* (4), 434-442.

16. Lowe, K., Perfluorinated blood substitutes and artificial oxygen carriers. *Blood Rev.* **1999,** *13* (3), 171-184.

17. Iyer, L. M.; Anantharaman, V.; Aravind, L., Ancient conserved domains shared by animal soluble guanylyl cyclases and bacterial signaling proteins. *BMC Genomics* **2003,** *4* (1), 5.

18. Boon, E. M.; Marletta, M. A., Ligand specificity of H-NOX domains: from sGC to bacterial NO sensors. *J. Inorg. Biochem.* **2005,** *99* (4), 892-902.

19. (a) Olea Jr, C.; Boon, E. M.; Pellicena, P.; Kuriyan, J.; Marletta, M. A., Probing the function of heme distortion in the H-NOX family. *ACS Chem. Biol.* **2008,** *3* (11), 703-710; (b) Schmidt, P. M.; Schramm, M.; Schröder, H.; Wunder, F.; Stasch, J.-P., Identification of residues crucially involved in the binding of the heme moiety of soluble guanylate cyclase. *J. Biol. Chem.* **2004,** *279* (4), 3025-3032.

20. Derbyshire, E. R.; Marletta, M. A., Structure and regulation of soluble guanylate cyclase. *Annu. Rev. Biochem.* **2012,** *81*, 533-559.

21. (a) Carlson, H. K.; Vance, R. E.; Marletta, M. A., H-NOX regulation of c-di-GMP metabolism and biofilm formation in Legionella pneumophila. *Mol. Microbiol.* **2010,** *77* (4), 930-942; (b) Henares, B. M.; Higgins, K. E.; Boon, E. M., Discovery of a nitric oxide responsive quorum sensing circuit in Vibrio harveyi. *ACS Chem. Biol.* **2012,** *7* (8), 1331-1336.

22. Pellicena, P.; Karow, D. S.; Boon, E. M.; Marletta, M. A.; Kuriyan, J., Crystal structure of an oxygen-binding heme domain related to soluble guanylate cyclases. *Proc. Natl. Acad. Sci.* **2004,** *101* (35), 12854-12859.

23. Boon, E. M.; Huang, S. H.; Marletta, M. A., A molecular basis for NO selectivity in soluble guanylate cyclase. *Nat. Chem. Biol.* **2005,** *1* (1), 53-59.

24. (a) Eich, R. F.; Li, T.; Lemon, D. D.; Doherty, D. H.; Curry, S. R.; Aitken, J. F.; Mathews, A. J.; Johnson, K. A.; Smith, R. D.; Phillips, G. N., Mechanism of NO-induced oxidation of myoglobin and hemoglobin. *Biochemistry* **1996,** *35* (22), 6976-6983; (b) Weinert, E. E.; Plate, L.; Whited, C. A.; Olea, C.; Marletta, M. A., Determinants of Ligand Affinity and Heme Reactivity in H-NOX Domains. *Angew. Chem. Int. Ed.* **2010,** *49* (4), 720-723.

25. Boon, E. M.; Marletta, M. A., Sensitive and selective detection of nitric oxide using an H-NOX domain. *J. Am. Chem. Soc.* **2006,** *128* (31), 10022-10023.

26. Weinert, E. E.; Phillips-Piro, C. M.; Tran, R.; Mathies, R. A.; Marletta, M. A., Controlling Conformational Flexibility of an O2-Binding H-NOX Domain. *Biochemistry* **2011,** *50* (32), 6832-6840.

27. Capece, L.; Marti, M. A.; Crespo, A.; Doctorovich, F.; Estrin, D. A., Heme protein oxygen affinity regulation exerted by proximal effects. *J. Am. Chem. Soc.* **2006,** *128* (38), 12455-12461.

28. Karow, D. S.; Pan, D.; Tran, R.; Pellicena, P.; Presley, A.; Mathies, R. A.; Marletta, M. A., Spectroscopic characterization of the soluble guanylate cyclase-like heme domains from Vibrio cholerae and Thermoanaerobacter tengcongensis. *Biochemistry* **2004,** *43* (31), 10203-10211.

29. DeSantis, G.; Wong, K.; Farwell, B.; Chatman, K.; Zhu, Z.; Tomlinson, G.; Huang, H.; Tan, X.; Bibbs, L.; Chen, P., Creation of a productive, highly enantioselective nitrilase through gene site saturation mutagenesis (GSSM). *J. Am. Chem. Soc.* **2003,** *125* (38), 11476-11477.

30. Erbil, W. K.; Price, M. S.; Wemmer, D. E.; Marletta, M. A., A structural basis for H-NOX signaling in Shewanella oneidensis by trapping a histidine kinase inhibitory conformation. *Proc. Natl. Acad. Sci.* **2009,** *106* (47), 19753-19760.

31. (a) Kretz, K. A.; Richardson, T. H.; Gray, K. A.; Robertson, D. E.; Tan, X.; Short, J. M., Gene site saturation mutagenesis: a comprehensive mutagenesis approach. *Methods Enzymol.* **2004,** *388*, 3-11; (b) Steffens, D. L.; Williams, J. G., Efficient site-directed

saturation mutagenesis using degenerate oligonucleotides. *J. Biomol. Tech* **2007,** *18* (3), 147.

32. Zheng, L.; Baumann, U.; Reymond, J.-L., An efficient one-step site-directed and site-saturation mutagenesis protocol. *Nucleic Acids Res.* **2004,** *32* (14), e115-e115.

33. (a) Otey, C. R.; Landwehr, M.; Endelman, J. B.; Hiraga, K.; Bloom, J. D.; Arnold, F. H., Structure-guided recombination creates an artificial family of cytochromes P450. *PLoS Biol.* **2006,** *4* (5), e112; (b) Otey, C. R.; Silberg, J. J.; Voigt, C. A.; Endelman, J. B.; Bandara, G.; Arnold, F. H., Functional evolution and structural conservation in chimeric cytochromes P450: calibrating a structure-guided approach. *Chem. Biol.* **2004,** *11* (3), 309-318.

34. Heim, R.; Prasher, D. C.; Tsien, R. Y., Wavelength mutations and posttranslational autoxidation of green fluorescent protein. *Proc. Natl. Acad. Sci.* **1994,** *91* (26), 12501-12504.

35. Ai, H.-w.; Shaner, N. C.; Cheng, Z.; Tsien, R. Y.; Campbell, R. E., Exploration of new chromophore structures leads to the identification of improved blue fluorescent proteins. *Biochemistry* **2007,** *46* (20), 5904-5910.

36. Jeong, J.-Y.; Yim, H.-S.; Ryu, J.-Y.; Lee, H. S.; Lee, J.-H.; Seen, D.-S.; Kang, S. G., One-step sequence-and ligation-independent cloning as a rapid and versatile cloning method for functional genomics studies. *Appl. Environ. Microbiol.* **2012,** *78* (15), 5440-5443.

37. Bonner, W.; Hulett, H.; Sweet, R.; Herzenberg, L., Fluorescence activated cell sorting. *Rev. Sci. Instrum.* **1972,** *43* (3), 404-409.

38. (a) Colin, M.; Moritz, S.; Schneider, H.; Capeau, J.; Coutelle, C.; Brahimi-Horn, M., Haemoglobin interferes with the ex vivo luciferase luminescence assay: consequence for detection of luciferase reporter gene expression in vivo. *Gene Ther.* **2000,** *7* (15), 1333; (b) Yang, N.-C.; Ho, W.-M.; Chen, Y.-H.; Hu, M.-L., A convenient one-step extraction of cellular ATP using boiling water for the luciferin–luciferase assay of ATP. *Anal. Biochem.* **2002,** *306* (2), 323-327.

39. Wilson, T.; Hastings, J. W., Bioluminescence. *Annu. Rev. Cell Dev. Biol.* **1998,** *14* (1), 197-230.

40. Nakatsu, T.; Ichiyama, S.; Hiratake, J.; Saldanha, A.; Kobashi, N.; Sakata, K.; Kato, H., Structural basis for the spectral difference in luciferase bioluminescence. *Nature* **2006,** *440* (7082), 372-376.

41. Arain, S.; Weiss, S.; Heinzle, E.; John, G. T.; Krause, C.; Klimant, I., Gas sensing in microplates with optodes: influence of oxygen exchange between sample, air, and plate material. *Biotechnol. Bioeng.* **2005,** *90* (3), 271-280.

42. Truesdale, G.; Downing, A.; Lowden, G., The solubility of oxygen in pure water and sea-water. *J. App. Chem.* **1955,** *5* (2), 53-62.

43. Van Der Merwe, P. A., Surface plasmon resonance. *Protein–ligand interactions: hydrodynamics and calorimetry. Oxford University Press, Oxford* **2001**, 137-170.

44. Marti, M. A.; Crespo, A.; Capece, L.; Boechi, L.; Bikiel, D. E.; Scherlis, D. A.; Estrin, D. A., Dioxygen affinity in heme proteins investigated by computer simulation. *J. Inorg. Biochem.* **2006,** *100* (4), 761-770.

45. Zhou, M.; Diwu, Z.; Panchuk-Voloshina, N.; Haugland, R. P., A stable nonfluorescent derivative of resorufin for the fluorometric determination of trace hydrogen peroxide: applications in detecting the activity of phagocyte NADPH oxidase and other oxidases. *Anal. Biochem.* **1997,** *253* (2), 162-168.

46. (a) Palamakumbura, A. H.; Trackman, P. C., A fluorometric assay for detection of lysyl oxidase enzyme activity in biological samples. *Anal. Biochem.* **2002,** *300* (2), 245-251; (b) Rhee, S. G.; Chang, T.-S.; Jeong, W.; Kang, D., Methods for detection and measurement of hydrogen peroxide inside and outside of cells. *Mol. Cells* **2010,** *29* (6), 539-549.

47. Mazura, P.; Fohlerová, R.; Brzobohatý, B.; Kiran, N. S.; Janda, L., A new, sensitive method for enzyme kinetic studies of scarce glucosides. *J. Biochem. Biophys. Methods* **2006,** *68* (1), 55-63.